

HIGH-LATITUDE IONOSPHERIC CONVECTION PATTERNS DEPENDENT ON THE IMF ORIENTATION

L.I. Gromova¹, J.A. Cumnock^{2,3}, L.G. Blomberg², S. Eriksson⁴, A.E. Levitin¹, Y.I. Feldstein¹

¹*Institute of Terrestrial Magnetism, Ionosphere and Radio Wave Propagation, Troitsk, Moscow Region, Russia*

²*Space and Plasma Physics, School of Electrical Engineering, Royal Institute of Technology, Stockholm, Sweden*

³*Center for Space Sciences, University of Texas at Dallas Laboratory for Atmospheric and Space Physics*

⁴*Laboratory for Atmospheric and Space Physics University of Colorado, Boulder*

Abstract. The IZMEM model provides high-latitude ionospheric plasma convection patterns in both hemispheres as a function of the IMF orientation. Model electric potentials are compared with electric field measurements from the DE2, FAST and DMSP satellites along high-latitude passes of the Northern and Southern hemispheres during IMF $B_z < 0$ and $B_y < 0$ ($B_y > 0$). It has been shown that the IZMEM model electric potentials are in good agreement with measurements along the satellite passes, which makes the IZMEM global spatial convection patterns for these plausible. For small IMF magnitude ionospheric convection patterns generally consist of two cells with a positive potential cell on the dawn-side and a negative potential cell on the dusk-side. For IMF $B_y < 0$ ($B_y > 0$) a positive (negative) potential cell becomes dominant in the northern hemisphere, and oppositely in the southern hemisphere. During $B_z > 0$ the convection pattern changes from the standard two-cell pattern to a more complicated one. IZMEM shows two additional convection cells in the dayside polar cap, positive (negative) potential cell is present duskward (dawnward) of the noon-midnight meridian, and may cause three-cell or four-cell convection pattern depending on B_y/B_z ratio.

Introduction

The IZMEM Electrodynamic Model (IZMEM) has been developed using a regression analysis of geomagnetic variations caused by IMF at high latitudes of northern [Feldstein and Levitin, 1986] and southern [Papitashvili et al., 1994] hemispheres. Using IMF components B_y and B_z as input parameters IZMEM model represents spatial-temporal distribution of geomagnetic variations, ionospheric current, ionospheric electric field, field-aligned currents and Joule heating over both northern and southern polar regions above $\phi = 60^\circ$ corrected geomagnetic latitudes. IZMEM model outputs have been compared with satellite observations and ground radar data [Dremukhina et al., 1998; Feldstein et al., 1994, 1996, 1998] and normalized by the experimental satellite data [Papitashvili et al., 1995].

Observation and IZMEM modelling

We consider the model convection patterns, the number of convection cells, and the possibility to verify them experimentally. Any description of the global high-latitude ionospheric convection is based on a certain hypothesis. Because of this and because of the complexity of the phenomenon, there is still no generally accepted description of the spatial configuration of the convection or the number of convection cells during northward IMF. As a result, components of complicated two-cells convection pattern may be interpreted as independent cells. Likewise, the ambiguity may result in the number of cells being underestimated.

Fig. 1 demonstrates high-latitude ionospheric plasma convection patterns provided by IZMEM model (left-side) and IZMEM electric potential in comparison with the potential calculated from electric field data along DE2 and FAST tracks (right-side) for moderate northward IMF when $|B_y|$ and B_z are less than 10 nT. Calculated potential from DE2 and FAST measurements are taken from Heelis et al. [1986] and Eriksson et al. [2002], respectively. For IMF $B_y < 0$ ($B_y > 0$) a positive (negative) potential cell becomes dominant in the polar region (see Fig. 1c and Fig. 1a). During $B_z > 0$ the convection pattern changes from the standard two-cell pattern to a more complicated one (see Fig. 1b). However, IZMEM results in a two-cell convection pattern for a moderate $B_z < 10$ nT. Figure 1 illustrates a rather good agreement between IZMEM model and calculated potential variation along the satellite tracks, which makes plausible the global spatial convection patterns. They were interpreted in [Heelis et al. 1986] as four-cells with four components marked I – IV (Fig. 1b).

Fig. 2 and Fig. 3 show electrostatic potential patterns generated by the IZMEM model at the time of DMSP F13 and F14 northern (Fig. 2) and southern (Fig. 3) hemisphere passes on 8 November 1998 as well as the comparison of modeled and measured potentials along the satellites tracks. Calculated potential from the DMSP F13 and F14 measurements are taken from Cumnock and Blomberg [2004] and Cumnock et al. [2006]. IZMEM potentials have been set to zero at the latitude 60° , and positive potentials along the some DMSP F14 tracks have been smoothed at the auroral latitudes.

Polar plots in Fig. 2 demonstrate two-cell convection pattern derived by winter IZMEM model for northern hemisphere during different IMF conditions: B_y changes from -1.1 nT (on the left) to -17.3 nT (on the right) and B_z

is strongly positive. As can be seen, during IMF $B_z \gg 0$ positive potential cell (solid line) dominates in the polar cap. In addition a negative potential cell (dotted line) is located on the dawnside of the polar cap. The positive cell grows in strength whereas the negative cell withdraws from the high-latitude region as B_y gets more negative.

Maximum (minimum) potentials are 54.49 kV (-46.06 kV) for $B_y = -1.1$ nT and 62.20 kV (-38.62 kV) for $B_y = -17.3$ nT. For $B_y = -17.3$ nT we have a counter-clockwise single lobe cell as expected for strongly negative IMF B_y with a strong Svalbard-Mansurov eastward flow at noon. Line plots of Fig.2b,c show satisfactory agreement between IZMEM and the calculated potential variation along DMSP tracks, but there is deviation of the model potentials from calculated ones. IZMEM derived from hourly mean values of the IMF and ground-based geomagnetic data using a regression analysis and therefore it does not take into account short-period variation of the IMF and geomagnetic fields. The height-integrated ionospheric conductivity model made for $K_p < 3$ and $K_p > 3+$ [Wallis, D.D., and Budzinski, E.E., 1981] have been applied for both hemispheres for quiet and disturbed IMF conditions respectively. It makes the conductivity model rough and deficient to describe large-scale and small-scale variations of the ionospheric conductivity.

Polar plots of Fig. 3 present ionospheric plasma convection patterns provided by summer IZMEM model for southern hemisphere as two-cell patterns for $B_z > 0$: positive cell on the dusk-side of the polar cap and negative cell on the dawn-side. The right dial shows that during small negative B_y the line dividing the two reverse convection cells is aligned along the noon-midnight meridian. When B_y changes to -16.2 nT the dividing line moves towards the dusk-side from the noon-midnight meridian (see the left dial) that is caused by dominating B_y -dependent cell with different direction of convection in the northern and southern hemispheres for the same sign of B_y . The discrepancy of the model potentials from those calculated from satellite measurements is more appreciable than for the northern hemisphere. The model amplitude is ~ 1.5 times larger than calculated one that may be caused by the transpolar potential saturation in the ionosphere during strong electric field in the solar wind [Ober et al., 2003 and references therein].

Discussion and conclusions

IZMEM model provides some independent elementary IMF-related high-latitude ionospheric plasma convection patterns. IMF-independent two-cell convection pattern φ_0 represents “background” potential which, exists in the ionosphere permanently and is controlled by quasi-viscous interaction of the solar wind with the magnetosphere. The other patterns are caused by IMF azimuthal (φ_y), northern (φ_{z+}) and southern (φ_{z-}) components. For any given IMF conditions the final pattern is a superposition of the elementary patterns. During northward IMF when $|B_y|$ and B_z are less than 10 nT vortices of φ_0 pattern is more intensive than vortices of φ_y and φ_{z+} patterns and the final convection pattern remains two-cell with positive (negative) potential cell downward (duskward) of the noon-midnight meridian, but it may be distorted (see Fig1a,b,c.). The B_y -dependent potential vortex of φ_y -pattern causes the asymmetry of convection in morning and evening cells only. This has been described in [Eriksson et al., 2002] when studying large-scale field-aligned currents. Vortices of φ_{z+} pattern distort potential cells (see Fig1b). During $B_z \gg 0$ vortices of φ_{z+} pattern became dominating and exceed vortices of φ_0 and φ_y patterns. As a result the standard two-cell convection pattern changes to a more complicated one with positive(negative) potential cell duskward (dawnward) of the noon-midnight meridian. Thus, the IZMEM model shows that two-cell large-scale convection patterns during IMF $B_z < 10$ nT and $B_z > 20$ nT are different from each other and four-cell or three-cell convection patterns are possible depending on B_y/B_z ratio.

Acknowledgments. This study is supported by RFBR grant 05-05-65196. The collaboration between IZMIRAN and the Royal Institute of Technology was supported by a grant from the Royal Swedish Academy of Sciences.

References

- Cumnock, J.A., and Blomberg, L.G., Transpolar arc evolution and associated potential patterns, *Annales Geophysicae*, 22, 1213, 2004.
- Cumnock, J.A., Blomberg, L.G., Alexeev, I.I., Belenkaya, E.S., Bobrovnikov, S.Yu., and Kalegaev, V.V., Simultaneous polar aurorae and modelled convection patterns in both hemispheres, *Adv.Space Res.*, 38, 1685, 2006.
- Dremukhina, L.A., Levitin, A.E., and Papitashvili, V.O., Analytical representation of IZMEM model for near-real time prediction of electromagnetic weather, *J. Atmos. Sol. Terr. Phys.*, 60, 1517, 1998.
- Eriksson, S., Bonnel, J.W., Blomberg, L.G., Ergun, R.E., Marklund, G.T., and Carlson, C.W., Lobe cell convection and field-aligned currents poleward of the region 1 current system, *J. Geophys. Res.*, vol.107, N A8, 1185, 10.1029/2001JA005041, 2002.
- Heelis, R. A., Reiff, P.H., Winningham, J.D., and Hanson, W.B., Ionospheric Convection Signatures Observed by DE 2 during Northward Interplanetary Magnetic Field, *J. Geophys. Res.*, 91, 5817, 1986.
- Feldstein Y.I. and Levitin A.E., Solar wind control of electric fields and currents in the ionosphere, *J. Geomagn. Geoelectr.*, v.38, N 11, 1143, 1986.
- Feldstein Y. I., Levitin, A.E., Gromova, L.I., Dremukhina, L.A., Blomberg, L.G., Lindqvist, P.-A., and Marklund, G.T., Electromagnetic weather at 100 km altitude on 3 August 1986, *Geophys. Res. Lett.*, 21, N19, 2095, 1994.
- Feldstein Y. I., Levitin, A.E., Gromova, L.I., Blomberg, L.G., Lindqvist, P.-A., and Marklund, G.T., Electromagnetic characteristics of high-latitude ionosphere during the various phases of magnetic storms, *J. Geophys. Res.*, 101, N9, 19921, 1996.

Feldstein, Ya. I., Gromova, L.I., Levitin, A.E., Papitashvili, V.O., Belov, B.A., Kustov, A.V., Sofko, G.J., Greenwald, R.A., and Ruohoniemi, M.J., Convection in high latitude ionosphere during non-steady orientation of the IMF: SuperDARN and IZMEM predictions, *Geomagn. Aeron.*, 38, No 4, 29, 1998.

Ober, D.M., Maynard, N.C., and Burke, W.J., Testing the Hill model of transpolar potential saturation with observations, *J. Geophys. Res.*, 108, N A12, 1467, doi:10.1029/2003JA010154, 2003.

Papitashvili, V. O., Belov, B.A., Faermark, D.S., Feldstein, Ya.I., S. A. Golyshev, S.A., Gromova, L.I., and Levitin, A.E., Electric potential patterns in the Northern and Southern polar regions parameterized by the interplanetary magnetic field, *J. Geophys. Res.*, 99, 13251, 1994.

Papitashvili, V.O., Clauer, C.R., Levitin, A.E., and Belov, B.A., Relationship between the observed and modeled modulation of the dayside ionospheric convection by the IMF B_y component, *J. Geophys. Res.*, 100, 7715, 1995

Wallis, D.D., and Budzinski, E.E., Empirical models of height integrated conductivities, *J. Geophys. Res.*, 86, 125, 1981.

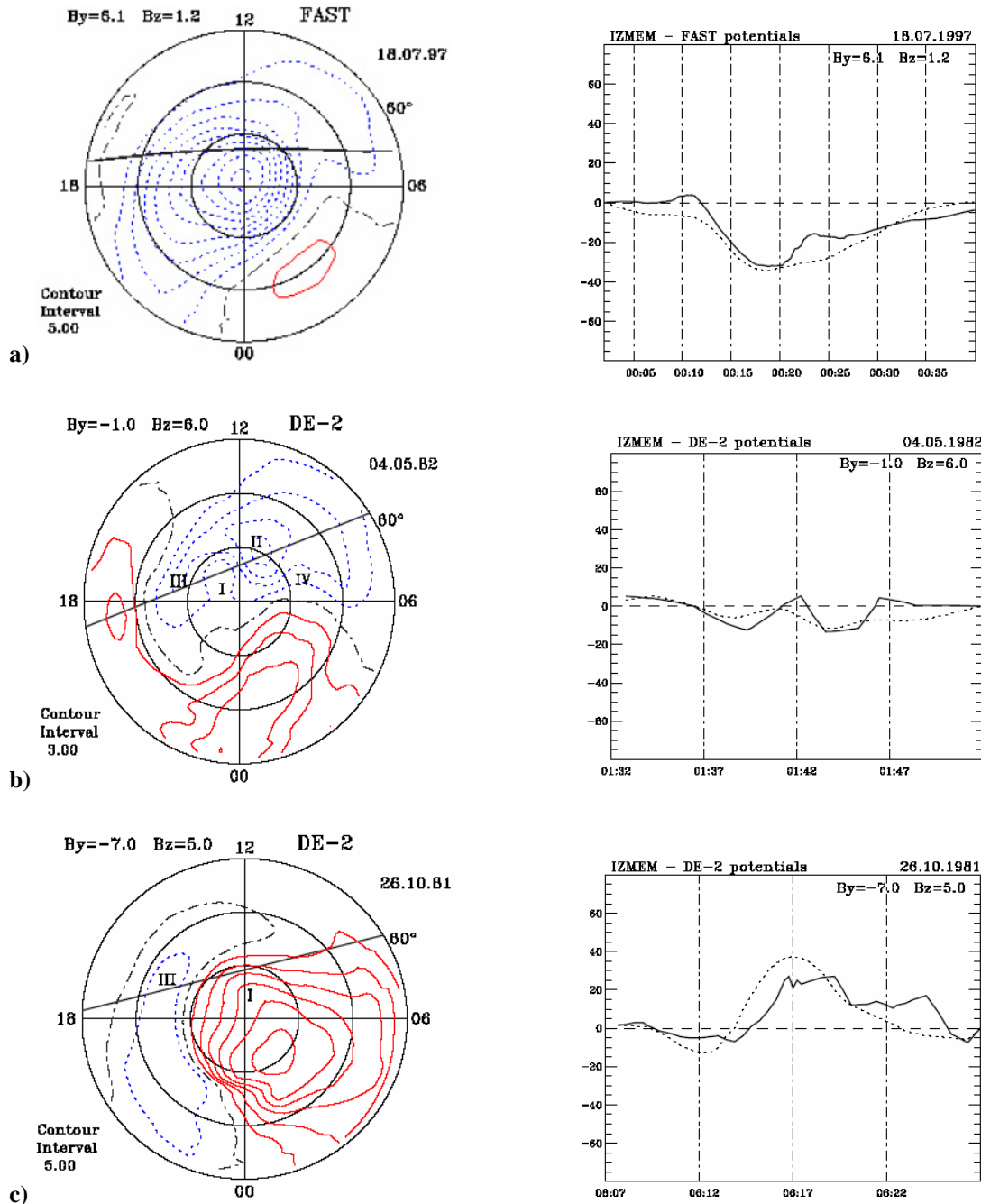


Figure 1. On the left: Modeled electrostatic potential patterns generated by the IZMEM model for the FAST and DE-2 satellites passes. The satellite tracks are also shown. FAST is flying from dawn to dusk, the DE-2 passes are from dusk to dawn. Polar plots are in the corrected geomagnetic latitude – magnetic local time coordinates. Positive (negative) potentials are shown by solid (dotted) lines. The dash-dot line denotes zero potential. Dates, IMF conditions, contour intervals are shown at each panel. On the right: Comparison of the measured (solid line) and calculated (dotted line) electrostatic potentials along the FAST and DE-2 satellites tracks.

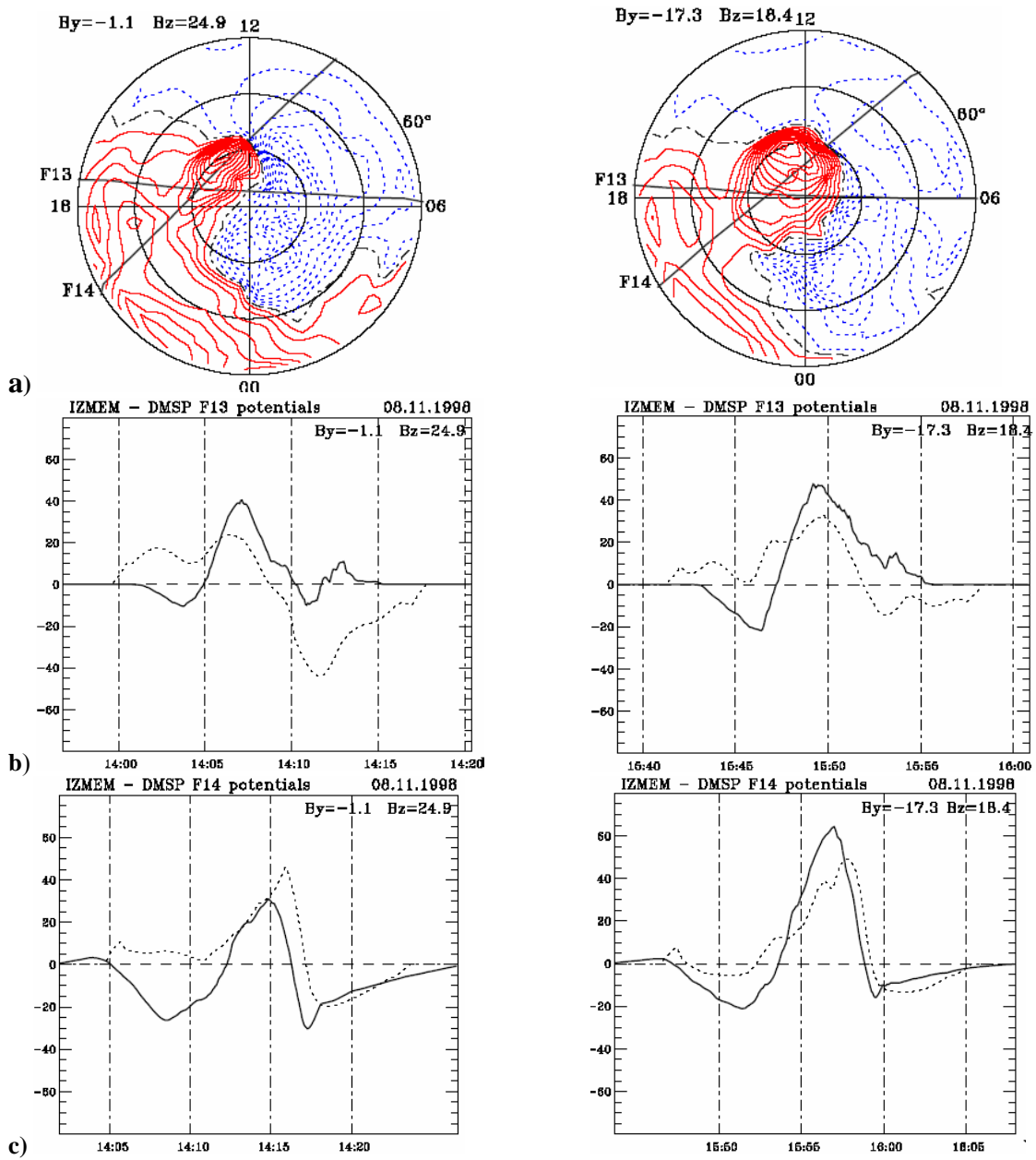


Figure 2. Electrostatic potential patterns (5 kV contour separation) generated by IZMEM model for DMSP F13 and F14 passes over Northern Hemisphere (a) and comparison of the electrostatic potentials along the satellite track calculated from satellite measurements (solid line) with those obtained from the model (dotted line). Polar plots are the same as in **Figure 1**. IMF conditions are shown at each panel.

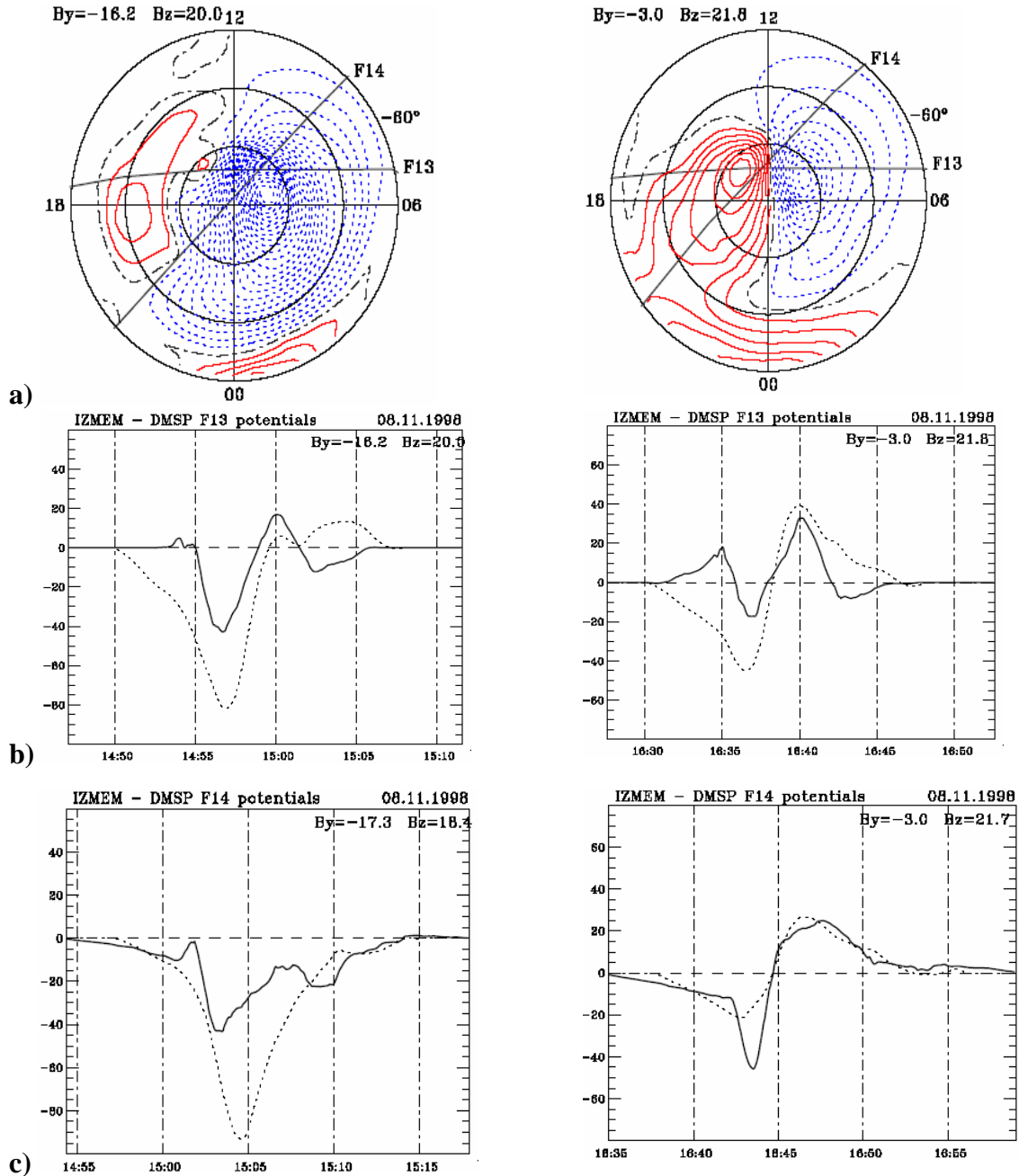


Figure 3. The same as Figure 2, but for satellite passes over Southern Hemisphere.